

PAPER • OPEN ACCESS

## Flow quality analysis of the TA-2 wind tunnel

To cite this article: M L C C Reis *et al* 2018 *J. Phys.: Conf. Ser.* **1065** 072034

View the [article online](#) for updates and enhancements.



**IOP | ebooks™**

Bringing you innovative digital publishing with leading voices to create your essential collection of books in STEM research.

Start exploring the collection - download the first chapter of every title for free.

## Flow quality analysis of the TA-2 wind tunnel

M L C C Reis<sup>1,2,3</sup>, M C C Araújo<sup>2</sup>, M S Souza<sup>1</sup>, R R Santos<sup>3</sup>

<sup>1</sup>Instituto de Aeronáutica e Espaço, Pr. Mal. Eduardo Gomes, 50, CEP 12228904, Brasil

<sup>2</sup>Instituto Tecnológico da Aeronáutica, Pr. Mal. Eduardo Gomes, 50, CEP 12228900, Brasil

<sup>3</sup>Universidade de Taubaté, Rua Daniel Danelli s/n, CEP 12060440, Brasil

E-mail: marialuisamlccr@fab.mil.br

**Abstract.** A test campaign to analyse the flow quality of the TA-2 subsonic wind tunnel is under progress. The measurand is the airflow speed. The velocity uniformity and the boundary layer velocity profile at the wind tunnel test section must be known because they impact on the model test results. The measured parameters are static pressure, total pressure, and static temperature. The estimated parameters are density and velocity. The least squares method is used for curve fitting. The uncertainties associated with the measured and estimated parameters are evaluated according to the recommendations of the Metre Convention. The results are presented in such a way as to help the wind tunnel community, including experimentalists and customers, to visualize and to quantify the airflow condition. Data reduction revealed that the airflow velocity decreases from the entrance to the centre of the test section. The boundary layer is thicker at the floor, in comparison with the lateral walls.

### 1. Introduction

Wind tunnels are aerodynamic laboratories employed to solve aerodynamic problems. The flow in the tunnel circuit simulates real conditions encountered by a structure submitted to aerodynamic loads. The fluid can be a gas, such as air, helium and nitrogen, or water as in the case of hydrodynamic tunnels. Wind tunnel data collected during the stages of an aerodynamic project can save lives, time and money.

Wind tunnels are classified according to the speed range of the flow: they are subsonic, near sonic, transonic, supersonic and hypersonic. Reference [1] defines speed regimes based on the local Mach number,  $M$ , at a point in the flow field; the flow is subsonic if  $M < 1$ , sonic if  $M = 1$  and supersonic if  $M > 1$ . In reference [2], low speed wind tunnels operate at  $M < 0.5$ , near sonic at  $0.5 < M < 0.95$ , transonic at  $0.5 < M < 1.4$ , supersonic at  $1.4 < M < 5$  and hypersonic above  $M = 5$ .

Research conducted in wind tunnels includes the study of heat transfer to an aerodynamic surface, drag reduction for sport purposes, external flow over a body, aerodynamic phenomena such as shock and expansion waves and shock wave-boundary layer interactions, etc.

The measurement chain in a wind tunnel is composed of many instruments: aerodynamic balances, Pitot tubes, anemometers, microphones, flow visualization equipment as well as temperature, force and pressure sensors.

---

<sup>1</sup> To whom any correspondence should be addressed.



The models to be tested can vary from land to aerospace vehicles, marine vehicles, military devices, civil structures, oil rigs, wind generating equipment and surveillance vehicles.

As in any laboratory, the experimentalists must conduct instrument calibration. The fundamental quantities which characterize the flow field are pressure, velocity, density and temperature. The measured flow field parameters in a wind tunnel test section are total pressure,  $p_0$ , static pressure,  $p$ , dynamic pressure,  $q$ , total temperature,  $T_0$ , static temperature,  $T$ , and airspeed,  $V$ . They are input quantities to estimate the flow density,  $\rho$ , the similarity parameters Mach number,  $M$ , Reynolds number,  $Re$ , pressure coefficient,  $C_p$ , and force and moment coefficients,  $C_F$ ,  $C_m$ .

Besides instrument calibration, there is a further measurement activity to be carried out regularly by the wind tunnel personnel to enhance the metrological test data reliability: the analysis and control of the flow quality.

According to international wind tunnel standards, the spatial variations in the flow field parameters, the turbulence level, the boundary layer, acoustic characteristics and the transition Reynolds number must be under statistical control [3]. The flow angularity must also be considered.

Flow quality analysis requires an extensive testing program encompassing planning, execution, data acquisition, data reduction, and data storage. The schedule of the tests may be regular or vary due to changes in the wind tunnel circuit, hardware configuration and/or operational procedures [4]. When elaborating reports, authors should include information on raw data, measurement procedures, mathematical modelling, estimated parameters and associated uncertainties as well as comparison with past results, if available. The documentation is to be kept up-dated and available for operators and customers.

A detailed database can help to understand the flow field behavior and can be used to explain aerodynamic results originating from model testing and can reveal the need for improvement in the wind tunnel circuit.

The purpose of this paper is to present the methods employed at the TA-2 subsonic wind tunnel facility to verify the flow quality of the test section. The methods are in accordance with the international metrological community and aim to fulfill the requirements of test customers and test engineering staff in terms of description of the procedures, mathematical modeling and data presentation. The spatial variation of the flow field velocity at the TA-2 test section is provided. The boundary layer profile at the central locations of the upper, lower and lateral walls are also presented. The uncertainties associated with the measured and calculated parameters are estimated by using standardized recommendations [5, 6]. Boundary layer surveys in a wind tunnel can help identify the presence of airflow separation as well as defining the necessary gap to be kept between half-models and the walls.

## 2. Methods

The wind tunnel number 2, TA-2, is a subsonic, atmospheric, closed loop circuit wind tunnel. Built in the 1950's, it has contributed to development of aerodynamic projects for the Brazilian aeronautical sector and the construction industry. It is located in the Institute of Aeronautics and Space, Brazil.

The maximum airflow speed for an empty test section is around 138 m/s, *i.e.*, the maximum Mach number is approximately 0.40. The test section is 2.1 m high, 3.0 m wide and 3.2 m long. The airflow is driven by an 8.4 m diameter 7 blade fan connected to a motor drive. The engine power is 1.2 Megawatts with 400 revolutions per minute. The model strut provides an angle of attack up to 30° and a turntable permits a yaw angle of  $\pm 45^\circ$ .

For the present study, a Rake composed of fifteen Pitot tubes was placed in 25 different positions inside the test section, encompassing 5 cross-section areas; the first is named P1P2P3P4P5, the second P6P7P8P9P10 and so on (figure 1). The positions of the tubes are  $z$  equal to 1.982, 1.851, 1.720, 1.590, 1.459, 1.329, 1.198, 1.067, 0.937, 0.806, 0.676, 0.545, 0.415, 0.283 and 0.153 m from the test section floor. Values of  $y$  are -1.2, -0.6, 0, 0.6 and 1.2 m. Values of  $x$  are -1.6, -0.8, 0, 0.8 and 1.6 m. For example, the coordinates of P1 are (-1.6, -1.2, 0) m, P2 (-1.6, -0.6, 0) m, P3 (-1.6, 0, 0) and so on. Point P13 corresponds to the origin of the coordinate axes  $(x, y, z) = (0, 0, 0)$ .

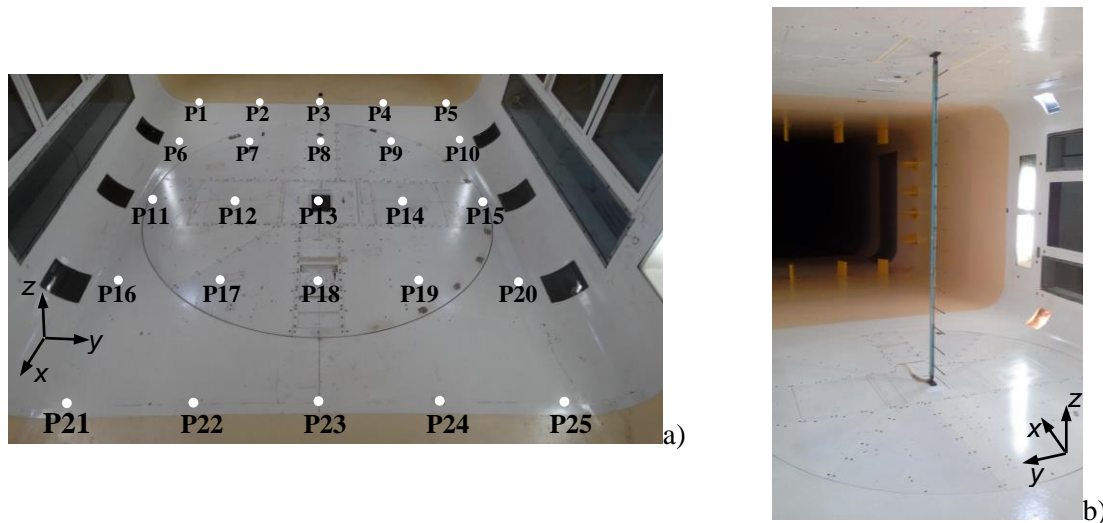


**Figure 1.** a) Stations at the TA-2 test section where the Rake is positioned. b) Rake positioned at P13 of the TA-2 test section. Positive  $x$  axis indicates flow direction.

A previous study [7] showed the flow uniformity at the central cross-section area, corresponding to tests carried out at locations P11, P12, P13, P14 and P15. The results shown here complement the previous work analysing the airflow behaviour at stations upstream and downstream of the central area and establish the relationship between the different stations.

For the boundary layer velocity profile analysis, a rake containing sixteen total pressure tubes was employed. The lowest tube is 1.7 mm from the floor and the highest is 103.2 mm (figure 2a). The points on the test section walls where the boundary layer was analysed are presented in figure 2b. They are aligned to the central cross-section and are named p26 (left side lateral wall), p27 (ceiling), p28 (right side lateral wall) and p29 (floor); p29 is coincident with P13. Both rakes were displaced in such a manner to diminish their interference during the tests.

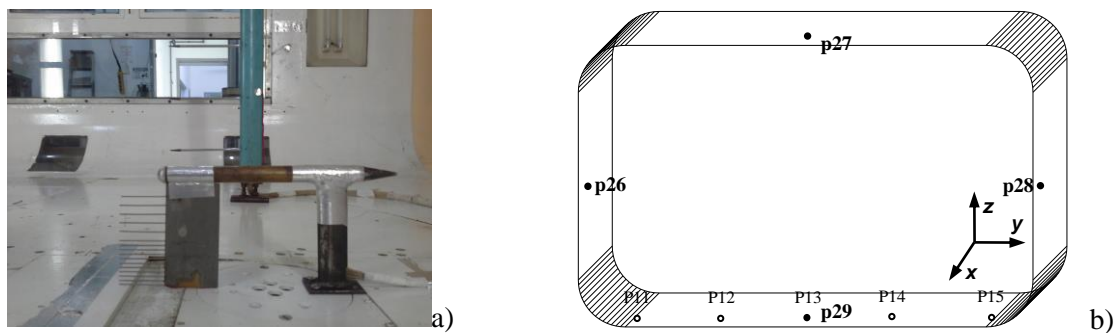


**Figure 2.** Boundary layer measurement. a) Test arrangement. b) Positioning.

### 3. The Mathematical Modelling

The flow in the TA-2 wind tunnel is air. For the subsonic regime, air properties behave as a perfect gas, so that the density,  $\rho$ , static pressure,  $p$ , and static temperature,  $T$ , are related to the equation of state:

$$p = \rho RT \quad (1)$$

where  $R$  is equal to 278 J/(kg.K) for air at standard conditions.

The density is evaluated at the test section entrance and corresponds to the free stream condition density. In this study, the flow is treated as one-dimensional, irrotational, incompressible and inviscid. Parameters  $\rho$  and  $T$  are taken as constant values with no friction, thermal conduction or diffusion [1].

The velocity,  $V$ , at a point of the airflow can be estimated from Bernoulli's equation, which is derived from Newton's second law applied to an elemental mass [8]:

$$p_0 = p + \frac{1}{2} \rho V^2 \quad (2)$$

where  $p_0$  is the total pressure.

The law of propagation of uncertainty is applied to equations (1) and (2) to estimate the uncertainties associated with the density and velocity quantities [5]:

$$u_\rho^2 = \left( \frac{1}{RT} \right)^2 u_p^2 + \left( \frac{-p_\infty}{RT^2} \right)^2 u_T^2 \quad (3)$$

$$u_V^2 = \left( \frac{1}{\rho} \left[ \frac{2(p_0 - p)}{\rho} \right]^{-\frac{1}{2}} \right)^2 u_{p_0}^2 + \left( \frac{-1}{\rho} \left[ \frac{2(p_0 - p)}{\rho} \right]^{-\frac{1}{2}} \right)^2 u_p^2 + \left( \frac{(p - p_0)}{\rho^2} \left[ \frac{2(p_0 - p)}{\rho} \right]^{-\frac{1}{2}} \right)^2 u_\rho^2 \quad (4)$$

The least squares method is used to fit first order polynomials,  $V = a_0 + a_1 z$ , to the local velocities to evaluate the vertical velocity uniformity in the studied cross-section areas [9, 10]. Ideally, the fitted first degree polynomials should present a null slope, *i.e.*,  $a_1 = 0$ . The uncertainty limits of the fitted curves are also estimated.

#### 4. Results and discussions

Codes in MatLab® and Excel® worksheets were elaborated to present velocity distributions of the airflow at the cross-section areas of the TA-2 test section.

Figure 3a shows the velocity profile results related to the flow regime equal to 300 mmH<sub>2</sub>O, which corresponds to a nominal velocity of 80 m/s. Following the wind direction, the sequence of the five cross-sections are located at  $x = -1.6, -0.8, 0.0, +0.8$  and  $+1.6$  m. When facing the flow, one observes that the airflow is faster at the entrance of the test section, *i.e.*, the velocity values are higher at  $x = -1.6$  m. At this region, the velocity values are greater at the negative part of the  $y$  axis. The velocity distribution becomes more uniform downstream the airflow.

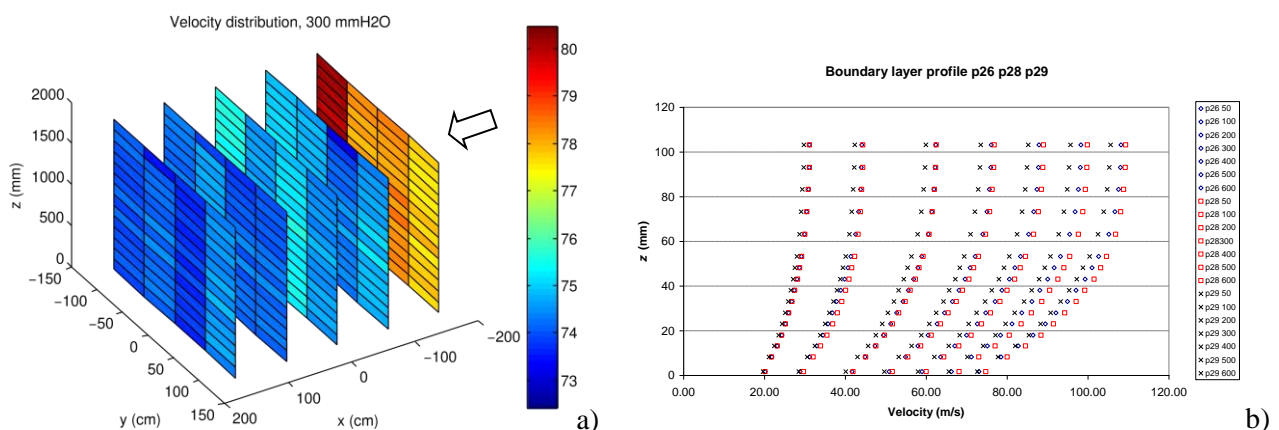


**Figure 3.** a) Velocity shown as color intensity (unit: m/s). b) Boundary layer velocity profiles.

Besides the color intensity representation of the velocity distribution, the results are also represented as curve fitting. As an example, for the regime equal to 300 mmH<sub>2</sub>O and position P5 next to the right lateral wall, the velocity at any vertical position can be quantified inserting the  $z$  value (in

millimeters) to the equation  $V = 77.909(0.026) - 53(22) \times 10^{-6}z$ . For P3, the polynomial becomes  $V = 78.22(0.07) + 1(5) \times 10^{-5}z$ . At the left lateral side, P1, it is  $V = 80.25(0.05) - 7(4) \times 10^{-5}z$ .

The boundary layer velocity profiles at the left lateral wall, p26, right lateral wall, p28, and floor, p29, are sketched in figure 3b, for all airflow regimes covered in the wind tunnel tests. Data reduction revealed that the boundary layer at the TA-2 test section is slightly thicker at the floor, *i.e.*, the velocity reaches the freestream condition later in comparison to the lateral walls. This can not be seen in figure 3b, but 98% of the freestream velocity is obtained at  $z = 53.3$  mm for p26 and p28. This condition occurs at  $z = 83.3$  mm for p29.

## 5. Conclusions

The airflow quality at the TA-2 test section was analysed. Data reduction was performed according to metrological guides.

The results were presented both qualitatively and quantitatively. For the former, the velocity was shown as color intensity. For the latter, curve equations were supplied. The vertical gradients were provided by the slope of the curves.

When reaching the central region of the test section, one observes an enhanced uniformity of the airflow, as expected, because wind tunnels are projected to have a laminar airflow at the region where the test model will be positioned.

At the central region, the floor of the test section has a thicker boundary layer in relation to the lateral walls. A possible cause of this effect can be the shape of the contraction section and imperfections such as gaps and steps on the locations occupied by the model support and the turntable.

This study can help experimental aerodynamicists to propose improvements in the wind tunnel circuit and to develop methods for wall interference corrections.

## 6. References

- [1] Anderson Jr J D 2001 *Fundamentals of Aerodynamics* (New York Mc Graw Hill) p 892
- [2] Pope A 1961 AGARDograph 54 Wind Tunnel Calibration Techniques (Advisory Group for Aeronautical Research and Development)
- [3] AIAA R-093-2003 Recommended Practice: *Calibration of Subsonic and Transonic Wind Tunnels* (American Institute of Aeronautics and Astronautics)
- [4] Henderson Jr A and McKinney L W 1993 NASA TP-3393 *Overview of the 1989 Wind Tunnel Calibration Workshop*
- [5] BIPM/JCGM 100:2008 *Evaluation of measurement data – Guide to the expression of uncertainty in measurement – GUM 1995 with minor corrections* (Joint Committee for Guides in Metrology, BIPM, Metrologia, IEC, IFCC, ILAC, ISO, IUPAC, IUPAP and OIML) p 120
- [6] BIPM/JCGM 200:2012 *International vocabulary of metrology – Basic and general concepts and associated terms (VIM)* (Joint Committee for Guides in Metrology, BIPM, Metrologia, IEC, IFCC, ILAC, ISO, IUPAC, IUPAP and OIML) p 91
- [7] Reis M L C C, Souza, M S Araujo 2017 *Proc. TC1-TC7-TC13 IMEKO-Rio Analysis of the airflow in the TA-2 subsonic wind tunnel*
- [8] Barlow J B, Rae Jr W H and Pope A 1999 *Low-Speed Wind Tunnel Testing* (John Wiley & Sons Inc.) p 713
- [9] Press W H, Teukolsky B P T, Vetterling W T 1990 *Numerical Recipes* (Cambridge University Press) chapter 14 pp 547–565
- [10] Bevington P R and Robinson D K 2003 *Data Reduction and Error Analysis for Physical Sciences* (New York Mc Graw Hill Higher Education) p 320